Electronic Supplementary Material (ESI) for RSC Advances.

Supporting Information

Flexible carbon nanofiber sponges for highly efficient and recyclable oil absorption

Xiang Ge,[a] Wei Yang,[a] Jitong Wang,[a] Donghui Long, *[a] Licheng Ling [a, b] and Wenming Qiao *[a, b]

[a] *State Key Laboratory of Chemical Engineering, East China University of Science and Technology, Shanghai 200237, China*

[b] *National Engineering Research Center of Ultrafine Powder, Shanghai 200231, China*

Content:

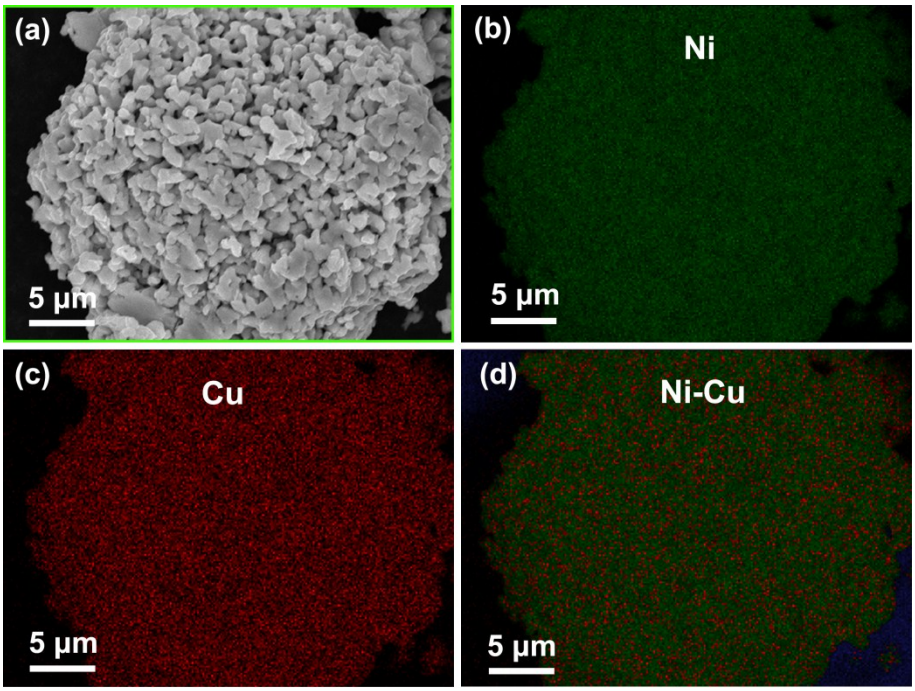

Figure S1 SEM mapping of Ni-Cu 8/2 catalyst. (a) SEM image of Ni-Cu catalyst, (b) Element Ni, (c) Element Cu, (d) Ni-Cu alloy.

The SEM elemental mapping images show matched spatial distributions of elements Ni and Cu, indicating the uniform distribution of Cu within the Ni matrix.

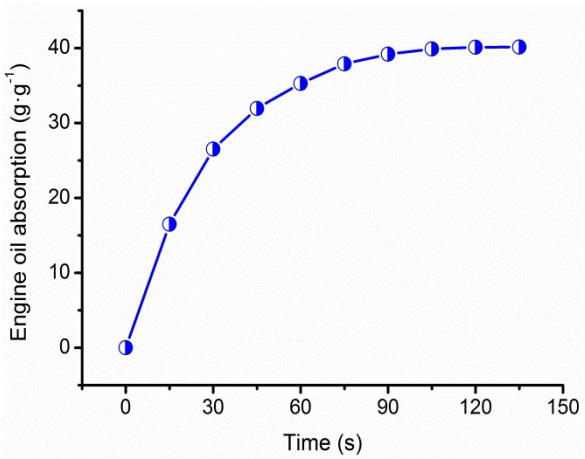

Figure S2 The variation of engine oil absorption capacity with respect to absorption time (CNF sponge density: 0.02 $g \cdot cm^{-1}$).

The absorption was very fast and typically reached saturation within 2 minutes by immersing the cylinders into the liquid. Therefore, the CNF sponges were immersed into the oils for 5 minutes to make sure that the materials were filled with oils.

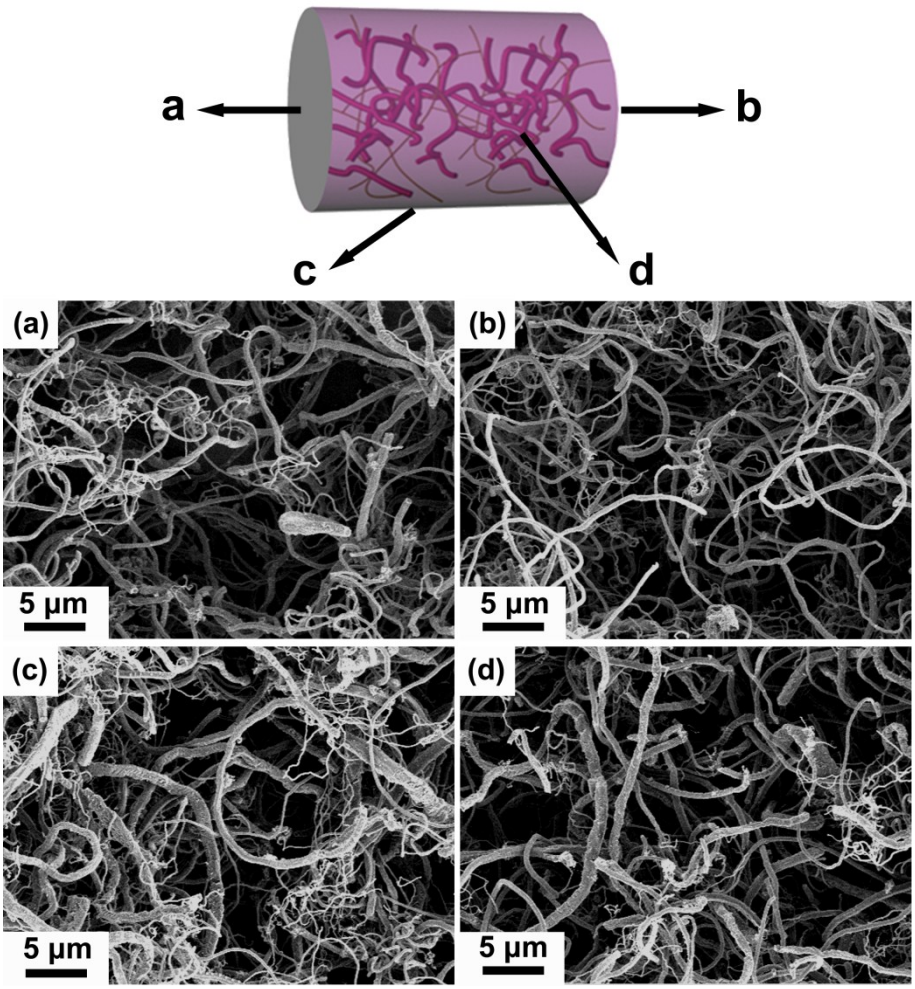

Figure S3 Comparison of morphologies in different regions of the CNF sponge (0.02 g·cm^{-3}). (a) Top surface, (b) Bottom surface, (c) Side wall, (d) Interior.

There are no obvious differences observed in the morphology from top surface to side-wall and to central region, indicating the uniformity of the CNF sponge.

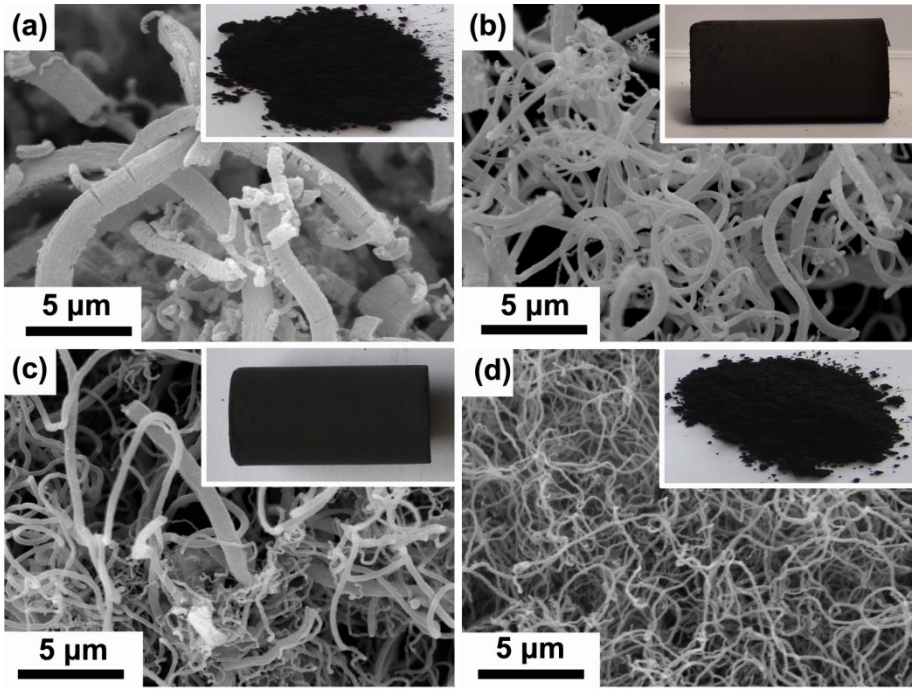

Figure S4 Comparison of microscopic and macroscopic (the insets) morphologies of CNFs synthesized with different catalysts. (a) Pure Ni, (b) Ni-Cu 8/2, (c) Ni-Cu 7/3, (d) Ni-Cu 5/5.

Only Ni-Cu with a narrow range of Cu content (20 ~ 30 wt.%) can grow the CNF sponges in this work. For the cases where pure Ni catalyst or alloy catalyst with high Cu content (~50 wt.%) are used, only CNF powders could be obtained from each catalyst. SEM images indicate that the CNFs produced from pure Ni catalyst consist of short and thick CNFs, while the CNFs from high-Cu-content alloy are composed of uniform thin CNFs, both of them lack the reinforcing rod-binding wire structure.

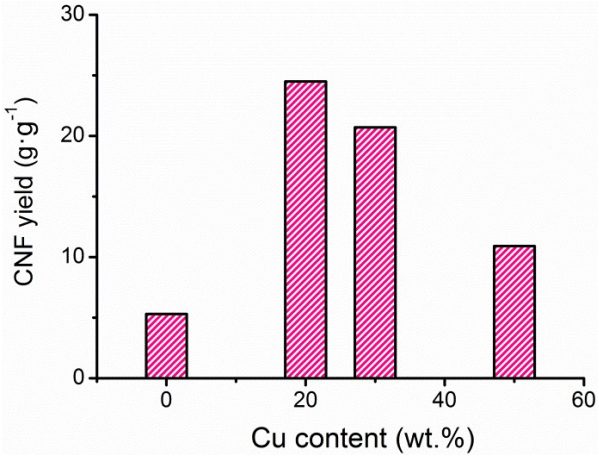

Figure S5 Variation of CNF yield with Cu content in the catalysts.

The CNF yields of the pure Ni and Ni-Cu 5/5 are significantly lower than that of Ni-Cu 8/2 and Ni-Cu 7/3 catalyst at the same growth conditions. These results suggest the unique Ni-Cu catalyst is the key to form 3D interconnected CNF networks.

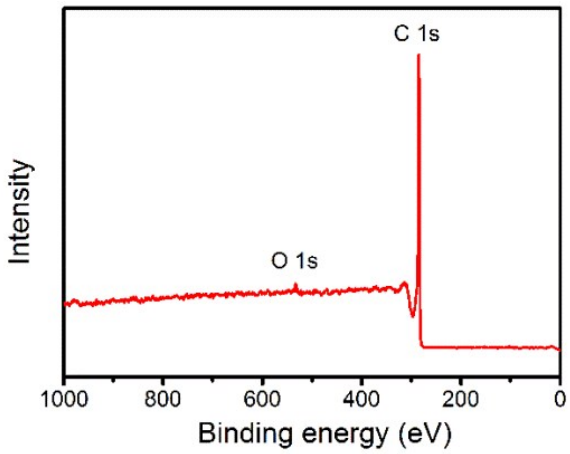

Figure S6 XPS spectra of the CNF sponge (density: 0.02 g·cm^{-3}).

The XPS spectra of the CNF sponge (density: 0.02 g·cm^{-3}) shows typical asymmetric peaks in the C 1s region. The atomic concentrations are 98.96% and 1.04% for C 1s and O 1s, respectively. Since the CNFs are prepared by oxygen-free CVD process, the trace oxygen atoms present on the CNF surface may be issued from surface residue or contaminants. Therefore, CNF sponges possess an inert, hydrophobic nature that is favor for oil adsorption.

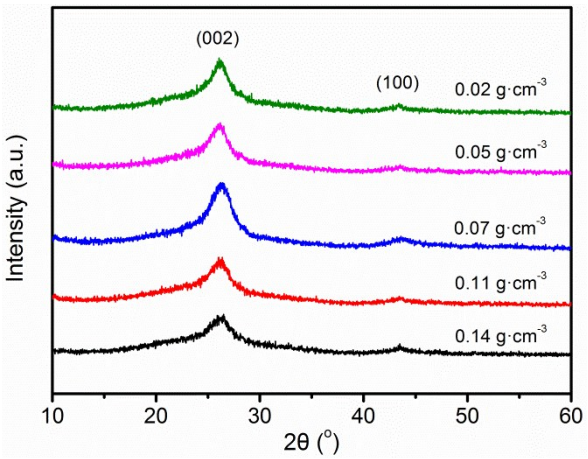

Figure S7 XRD patterns of CNF sponges with different densities.

All materials showed a prominent reflexion at ca. 26° and a weak peak at ca. 43 ° assigned to graphitic carbon (planes 002 and 100, respectively). No significative changes in reflexions assigned to graphitic carbon were observed among the CNF sponges with different densities.

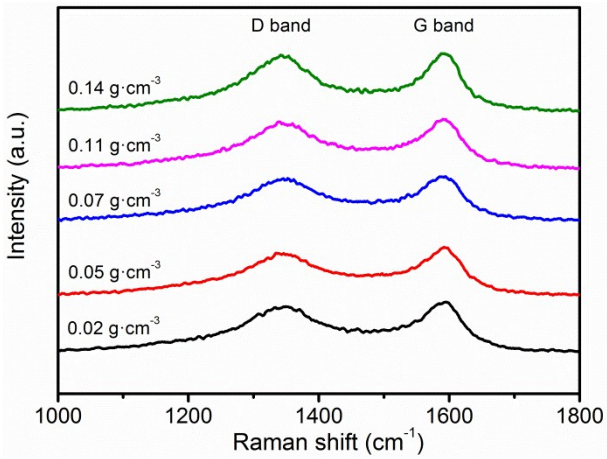

Figure S8 Raman spectra of CNF sponges with different densities.

The information about the graphitic crystalline structure and the amorphous carbon or defects on CNF sponges was acquired from Raman spectra. The bands at around 1590 cm^{-1} and 1344 cm^{-1} correspond to the high crystalline graphite vibration in the tangential stretching mode (graphitic lattice mode E2g) and the disorder induced phonon mode, which originates from the mode of boundaries in Brillouin zone, respectively. There is very little change in Raman spectra for CNF sponges with different densities.